Inducing New Crystal Structures through Random Copolymerization of Biodegradable Aliphatic Polyester

Xiangyang Li,[†] Jie Sun,[‡] Youju Huang,[†] Yong Geng,[§] Xiao Wang,[†] Zhe Ma,[†] Chunguang Shao,[†] Xiao Zhang,[⊥] Chuanlu Yang,[§] and Liangbin Li*,[†]

National Synchrotron Radiation Lab and Department of Polymer Science and Engineering, University of Science and Technology of China, Hefei, China; Institute of Chemistry Materials, China Academy of Engineering Physics, Mianyang, China; Department of Physics and Electrons, Ludong University, Yantai, China; and Department of Biology, University of Science and Technology of China, Hefei, China

Received December 30, 2007; Revised Manuscript Received February 19, 2008

ABSTRACT: The crystal structures of poly(hexamethylene sebacate-*co*-hexamethylene adipate), P(HSe-*co*-HA), copolymers have been studied with Fourier transformation infrared spectroscopy (FTIR) and X-ray fiber diffraction. All characteristic FTIR absorption bands of the crystals of HSe and HA comonomers are present in all copolymers, and each copolymer has only one melt temperature, which supports that P(HSe-*co*-HA) copolymers cocrystallize in a whole range of comonomer compositions. In addition to peak shift, some new diffraction peaks were observed in X-ray fiber diffraction patterns of the copolymers, which correspond to new crystals with different unit cells from those of the homopolymers. The crystal structures of the copolymers were analyzed, which varied with the composition of HA and HSe comonomers. Interestingly, the lattice constants *c* of P(HSe-*co*-20 mol % HA) and P(HSe-*co*-35 mol % HA) crystals are even larger than those of either homopolymers, which implies a new length scale may be induced in the random copolymers. This supports the formation of new crystals instead of normal lattice distortion.

Introduction

Biodegradable polymers have been attracting considerable attention over recent decades because of their potential contributions to worldwide environmental issues.[1–3] A central issue for biodegradable polymer is to understand its structure−properties relationship. In addition to its inherent chemical nature, structures in nanometer and micrometer scales are also of importance on its mechanical and degradation properties, which have been taken into account in designing new biodegradable polymers.

Copolymerization is a generic tool to create new materials with desirable properties. Leibler's recent review advocates that block copolymer will be the future of the plastics industry, which leads to the era of polymer nanoalloy.[4] In this respect, random copolymer, resembling many biopolymers like protein, is expected to render polymer alloy on a molecular scale, which indeed has attracted polymer industry for many years. However, putting two different comonomers in one chain leads to some complexities in their phase behaviors. Crystallization and microphase separation may couple and compete with each other, which determines the final structure and the consequent mechanical and biodegradation properties.[5–10] Three choices may occur: (i) comonomers are miscible and remain in the amorphous state; (ii) comonomers are immiscible and microphase-separated, where each species of comonomers may crystallize separately or stay as amorphous; (iii) comonomers cocrystallize into isomorphism or isodimorphism states.[11] As the free energy penalty to accommodate a foreign comonomer in its three-dimensional periodic arrangement is large, comonomers in many copolymers cannot cocrystallize.[12–14] For example, Gan et al.[12] and Kuwabara et al.[14] showed that minor comonomers are generally excluded out from crystalline region and exist in amorphous state. Nevertheless, comonomers of some copolymers do cocrystallize.[15–26] For example, De Rosa et al.[16] studied the cocrystallization behavior of propene and 1-butene. With increasing content of 1-butene, the increase of *a* and *b* axes from the values of s-PP to those of s-PB indicates that the comonomers (propene or 1-butene) are included in the unit cells. Several aromatic and more recently aliphatic polyesters with different comonomer lengths have been reported to show cocrystallization behavior.[27–31] Comparing to comonomers with different lateral sizes, the misfit in crystals due to different comonomer lengths generally leads to large free energy penalty. A nonperiodic layers model was employed to describe the cocrystal of copolymer by Hanna and Windle,[30] while Wendling et al.[31] proposed a model including defect Gibbs free energy. In general, a single melting and a single crystallization peak are observed in the cocrystallizable copolymers, which adopt the crystal structures of either homopolymers with slightly lattice distortion instead of creating a new crystal structure.

In this work, we reported that aliphatic polyester random copolymers of hexamethylene sebacate and hexamethylene adipate (P(HSe-*co*-HA)) cocrystallize into new structures which are different from the crystal structures of both homo-HSe and homo-HA. The crystal structure of PHA and PHSe was reported by many groups.[32–34] An orthorhombic unit cell with parameters $a = 1.008$ nm, $b = 1.464$ nm, and $c = 1.683$ nm was assigned to PHA crystal, and a monoclinic unit cell with parameters $a = 0.544$ nm, $b = 0.73$ nm, $c = 2.2$ nm, and $\beta = 113.3°$ was for PHSe crystal.[33,34] The crystallization behavior and crystal structure of similar aliphatic polyesters have been systematically studied by groups of Puiggali and Doi.[35–41]

Cocrystallization of P(HSe-*co*-HA) copolymers in a whole range of comonomer compositions was first confirmed by FTTR. X-ray fiber diffraction revealed that crystal structures of P(HSe-*co*-HA) copolymers are different from those of their homopolymers and vary with the concentration of comonomers. Inter-

* Corresponding author. E-mail: lbli@ustc.edu.cn.
[†] National Synchrotron Radiation Lab and Department of Polymer Science and Engineering, University of Science and Technology of China.
[‡] China Academy of Engineering Physics.
[§] Ludong University.
[⊥] Department of Biology, University of Science and Technology of China.

10.1021/ma702888d CCC: $40.75
Published on Web 04/02/2008

Table 1. Molecular Parameters, Melting Temperatures, and Compositions of PHSe, PHA, and Their Copolymers

materials	M_n ($\times 10^4$)	melting point (°C)	HA comonomer compositions (mol %)
PHA	6.50	62	100
P(HSe-*co*-75 mol % HA)	4.53	50	75
P(HSe-*co*-55 mol % HA)	4.48	50	55
P(HSe-*co*-35 mol % HA)	2.53	55	35
P(HSe-*co*-20 mol % HA)	4.60	63	20
PHSe	4.58	72	0%

estingly, the lattice constants *c* of some P(HSe-*co*-HA) copolymers crystals are even larger than those of either homopolymer.

Experimental Section

Materials. A typical procedure for polymerization is as follows: hexanediol (23.6 g), decahydronaphthalene (60 mL), and different ratios between sebacic acid and adipic acid were put into a 250 mL three-neck flask with an oil−water separator. The catalyst stannous chloride (0.07 g) was added to the reactor under stirring and nitrogen. The flask was immersed into an oil bath, which was heated to 150−160 °C and kept for 1−2 h. And then the temperature was up to 190−200 °C. The polymerization was allowed to proceed for 8−12 h before being cooled to room temperature. After removing decahydronaphthalene, the product was dissolved in trichloromethane (100−150 mL). After being filtered, the solution was precipitated into methanol (400 mL). The final product was dried at 60 °C under vacuum for 24 h. With monodisperse polystyrenes as standard and using the PE200 apparatus, the relative molecular weights and their distributions of polyester samples were measured by gel permeation chromatography (GPC) at 40 °C with chloroform as an eluant at a flow rate of 1.0 mL/min. The compositions of the copolymer were determined by ^{1}HNMR techniques. ^{1}HNMR spectra were recorded (90 MHz for H) on a JEOL JNM-EX90 spectrometer, using tetramethylsilane (TMS) as an internal standard in deuteriochloroform ($CDC1_3$). HA comonomer composition have been worked out by the peaks at $\delta = 4.03$ ppm and $\delta = 1.34$ ppm. PHSe, PHA, P(HSe-*co*-75 mol % HA), P(HSe-*co*-55 mol % HA), P(HSe-*co*-35 mol % HA), and P(HS-*co*-20 mol % HA) were synthesized in this study. Note the number in the abbreviation represents the molar percentage of HA comonomer in the copolymer, while the HSe composition is naturally 100% minus the corresponding number. The degrees of randomness (DR) of all P(HSe-*co*-HA) copolymer are in the range 0.90−0.94 calculated by the resonance ratio between 4.0 and 4.1 ppm in ^{1}H NMR spectra.[21] The melting temperatures were measured by differential scanning calorimetry (DSC). The molecular parameters, compositions, and melting temperatures of PHSe, PHA, and their copolymers are listed in Table 1.

FTIR Spectroscopy. For IR study of the melting of PHSe, PHA, and their copolymers, samples with a thickness of about 50 μm were placed between two ZnSe windows as a sandwich configuration, which were fixed in a homemade temperature-controlled cell. In-situ IR spectra were collected by using a Bruker TENSOR 37 FTIR spectroscopy at a resolution of 4 cm^{-1}. The melting process was studied to find the characteristic absorption bands of PHSe and PHA and their copolymers crystals, during which a heating rate of 1 °C/min was employed.

Wide-Angle X-ray Diffraction (WAXD). Two-dimensional (2D) X-ray fiber diffraction patterns were collected with a mar345 image plate in the scattering angle range of $2\theta = 1°-47°$ (radiation of wavelength 0.1542 nm, Cu Kα). The WAXD data were measured at room temperature on PHSe, PHA, P(HSe-*co*-75 mol % HA), P(HSe-*co*-55 mol %HA), P(HSe-*co*-35 mol % HA), and P(HS-*co*-20 mol % HA) samples. The sodium chloride crystals were used for the calibration of the diffraction angle.

Results

FTIR Measurements. FTIR was first employed to check whether the copolymers cocrystallize. Through in-situ measurements of FTIR during a heating scan, the characteristic absorption bands of crystals were identified for PHSe and PHA. The infrared spectra of PHSe, PHA, and their copolymers at room temperature are presented in Figure 1, in which the characteristic absorption bands for PHSe and PHA crystals are indicated. These bands are also listed in Table 2 for the convenience of comparison. The 911, 922, and 1262 cm^{-1} bands appear in crystallized PHA but not in PHSe, which disappear above the melting point of PHA. Similarly the 857, 1220, and 1297 cm^{-1} bands appear in crystallized PHSe alone and disappear upon melting. Thus, 911, 922, and 1262 cm^{-1} bands can be taken to represent the ordered conformational bands of HA comonomer, while 857, 1220, and 1297 cm^{-1} bands represent that of HSe. Figure 1 shows all these characteristic bands of HSe and HA comonomers appear in all P(HSe-*co*-HA) copolymers, which indicate both comonomers can crystallize in all P(HSe-*co*-HA) copolymers. Do the two comonomers cocrystallize or crystallize separately? In both cases, the characteristic bands of two comonomers can coexist. To check this, the melting processes of the crystallized samples were measured by in-situ FTIR. If HSe and HA comonomers cocrystallize, only one melting temperature is expected, and vice versa. Figure 2 shows the intensity evolution of 1262 cm^{-1} (representing HA) and 1220 cm^{-1} (representing HSe) bands during a heating scan. The intensities of 1220 and 1262 cm^{-1} bands sharply drop down at one temperature in each copolymer. The melting points of P(HSe-*co*-75 mol % HA), P(HSe-*co*-55 mol % HA), P(HSe-*co*-35 mol % HA), and P(HSe-*co*-20 mol % HA) are 50, 50, 55, and 63 °C, respectively, which is consistent with DSC results. Evidently, HSe and HA comonomers cocrystallize in all P(HSe-*co*-HA) copolymers. Figure 3 plots the melting temperature vs the composition of HA

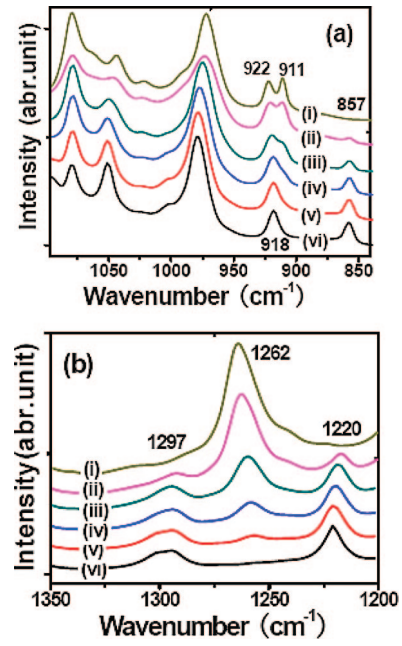

Figure 1. Comparison of the characteristic bands of (i) PHA, (ii) P(HSe-*co*-75 mol % HA), (iii) P(HSe-*co*-55 mol % HA), (iv) P(HSe-*co*-35 mol % HA), (v) P(HSe-*co*-20 mol % HA), and (vi) PHSe (a) in the 840−1100 cm^{-1} and (b) in the 1200−1350 cm^{-1} regions.

Table 2. Characteristic FTIR Absorption Bands of Crystallized PHSe and PHA

sample	characteristic peaks of crystalline (cm^{-1})
PHA	583, 735, 911, 922, 972, 1044, 1080, 1262, 1371, 1398, 1418, 1480
PHSe	583, 725, 754, 857, 918, 1049, 1096, 1180, 1220, 1297, 1361, 1378

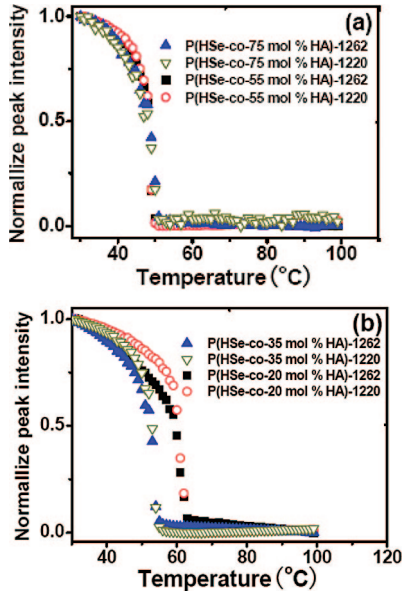

Figure 2. Intensity evolution of 1220 and 1262 cm^{-1} bands for (a) P(HSe-*co*-75 mol % HA) and P(HSe-*co*-55 mol % HA) and (b) P(HSe-*co*-35 mol % HA) and P(HSe-*co*-20 mol % HA) during a heating process with a heating rate of 1 °C/min.

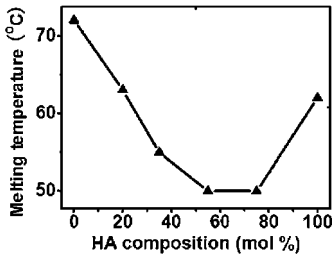

Figure 3. Plot of the melting temperatures of P(HSe-*co*-HA) copolymers vs the composition of HA comonomer.

monomer. An inflection point lays between the melting temperatures of P(HSe-*co*-75 mol % HA) and P(HSe-*co*-55 mol % HA). A rough extrapolation gives the minimum temperature around 45 °C with a HA composition of 65%.

WAXD Measurements. Though FTIR measurements show that cocrystallization occurs in all P(HSe-*co*-HA) copolymers, it cannot tell us the structures of the cocrystals, which require a tool more sensitive to long-range order. In order to obtain crystal structures of the cocrystallizable copolymers, two-dimensional X-ray fiber diffractions have been collected. We present the data for each copolymer in the following paragraphs.

PHA and PHSe. Before the investigation on the copolymers, the structures of the homopolymer PHA and PHSe were rechecked for the convenience of comparison. Figures 4 and 5 show the fiber diffraction patterns of PHA and PHSe, respectively. The diffraction patterns in Figures 4 and 5 correspond to a orthorhombic and a monoclinic structures, respectively, which have the same lattice parameters as reported by Puiggali et al.[33,34]

P(HSe-*co*-20 mol % HA). Figure 6 gives a 2D fiber diffraction pattern of P(HSe-*co*-20 mol % HA). Compared to PHSe, P(HSe-*co*-20 mol % HA) has two extra diffraction points. One diffraction point, corresponding to a spacing of 1.024 nm, lays in the meridional direction, while another is in the off-meridional direction, corresponding to a spacing of 0.512 nm. Additionally, two diffraction points of PHSe with spacing of 0.505 and 0.537 nm disappear in P(HSe-*co*-20 mol % HA). This unambiguously shows that the crystal

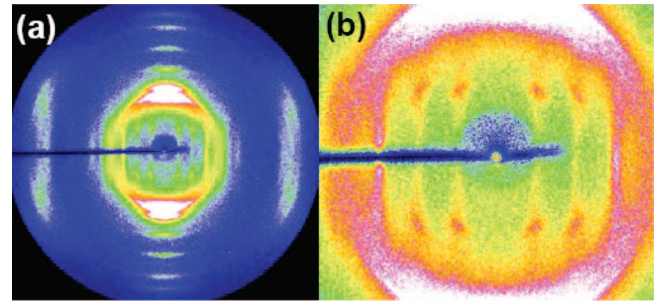

Figure 4. (a) Two-dimensional X-ray fiber diffraction pattern of PHA. (b) Partially enlarged diffraction pattern of PHA for the convenience to view the diffractions with small angle.

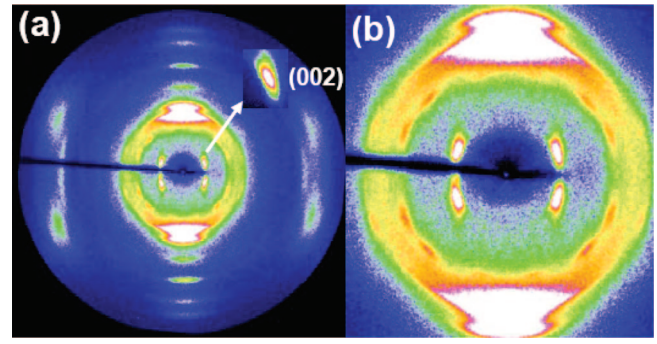

Figure 5. (a) Two-dimensional X-ray fiber diffraction pattern of PHSe. (b) Partially enlarged diffraction pattern of PHSe for the convenience to view the diffractions with small angle.

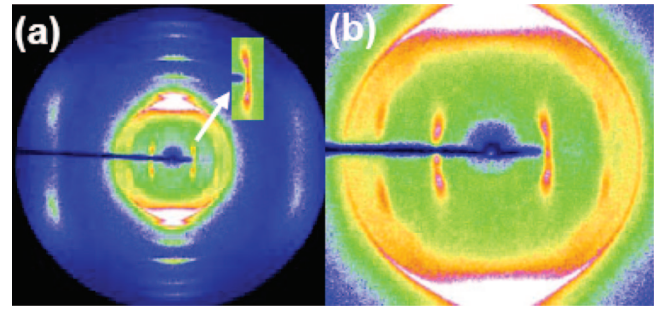

Figure 6. (a) Two-dimensional X-ray fiber diffraction pattern of P(HSe-*co*-20 mol % HA). (b) Partially enlarged diffraction pattern of P(HSe-*co*-20 mol % HA) for the convenience to view the diffractions with small angle.

structure of P(HSe-*co*-20 mol % HA) is different from that of PHSe. The pattern can be reasonably indexed assuming a monoclinic unit cell with parameters: $a = 1.185$ nm, $b = 1.464$ nm, $c = 2.321$ nm, and $\beta = 121.7°$. With this unit cell, the d spacing of different planes is calculated, which is compared with the experimental value in Table 3.

P(HSe-*co*-35 mol % HA). Figure 7 shows a 2D fiber diffraction pattern of P(HSe-*co*-35 mol % HA). The 2D fiber diffraction pattern of P(HSe-*co*-35 mol % HA) is similar to that of P(HSe-*co*-20 mol % HA). Nevertheless, the spacing of P(HSe-*co*-35 mol % HA) corresponding to $(10\bar{2})$ and $(20\bar{4})$ reflections are slight larger than those of P(HSe-*co*-20 mol % HA). The intensity of $(10\bar{2})$ diffraction is significantly stronger than that of P(HSe-*co*-20 mol % HA). On the basis of the diffraction pattern, a monoclinic unit cell is assigned with parameters $a = 1.191$ nm, $b = 1.46$ nm, $c = 2.424$ nm, and $\beta = 122.2°$. The experimental and calculated d spacings are listed in Table 4.

Table 3. Calculated and Experimental Spacings *d* (nm) of P(HSe-*co*-20 mol % HA) Copolymer[a]

index	d_{calc} (nm)	d_{measd} (nm)	
$10\bar{2}$	1.024	1.024	s M
002	0.987	0.987	s off M
$20\bar{4}$	0.512	0.512	m off M
220	0.415	0.414	vs E
040	0.366	0.366	vs E
240	0.296	0.295	m E
400	0.252	0.251	m E
420	0.238	0.238	w E
260	0.220	0.22	m E
440	0.208	0.207	m E
$30\bar{1}0$	0.231	0.232	w M
$41\bar{1}0$	0.220	0.218	m off M

[a] Based on a monoclinic unit cell with $a = 1.185$ nm, $b = 1.464$ nm, $c = 2.321$ nm, and $\beta = 121.7°$. Abbreviations denote that relative intensities and orientations: vs, very strong; s, strong; m, medium; w, weak; vw, very weak; M, meridional; E, equatorial; off M, off-meridional.

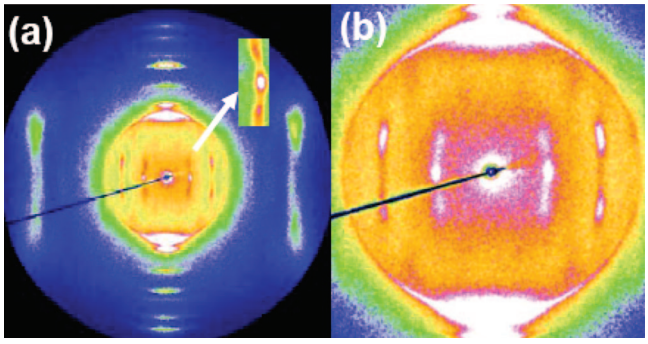

Figure 7. (a) Two-dimensional X-ray fiber diffraction pattern of P(HSe-*co*-35 mol % HA). (b) Partially enlarged diffraction pattern of P(HSe-*co*-35 mol % HA) for the convenience to view the diffractions with small angle.

Table 4. Calculated and Experimental Spacings *d* (nm) of P(HSe-*co*-35 mol % HA) Copolymer[a]

index	d_{calc} (nm)	d_{measd} (nm)	
$10\bar{2}$	1.055	1.055	s M
002	1.022	1.022	m off M
$20\bar{4}$	0.527	0.53	m off M
220	0.415	0.416	vs E
040	0.365	0.365	vs E
240	0.296	0.295	m E
400	0.252	0.253	vs E
420	0.238	0.238	w E
260	0.219	0.218	m E
440	0.207	0.207	w E
$40\bar{1}0$	0.231	0.232	m M
$30\bar{1}\bar{1}$	0.220	0.22	m off M
$40\bar{1}\bar{1}$	0.214	0.214	m off M

[a] Based on a monoclinic unit cell with $a = 1.191$ nm, $b = 1.46$ nm, $c = 2.424$ nm, and $\beta = 122.2°$. Abbreviations denote relative intensities and orientations: vs, very strong; s, strong; m, medium; w, weak; vw, very weak; M, meridional; E, equatorial; off M, off-meridional.

P(HSe-*co*-55 mol % HA). Figure 8 shows a 2D fiber diffraction pattern of P(HSe-*co*-55 mol % HA). The diffractions corresponding to large spacing such as (002) and ($10\bar{2}$) are weak or disappear compared to those of the copolymers with lower HA concentration. The spacing of P(HSe-*co*-55 mol % HA) corresponding to (004) reflections are slight larger than ($20\bar{4}$) of P(HSe-*co*-35 mol % HA). On the basis of the diffraction pattern, a monoclinic unit cell is assigned with parameters $a = 1.018$ nm, $b = 1.46$ nm, $c = 2.161$ nm, and $\beta = 98°$. The experimental and calculated *d* spacings are summarized in Table 5.

P(HSe-*co*-75 mol % HA). Figure 9 shows a 2D fiber diffraction pattern of P(HSe-*co*-75 mol % HA). Copolymerizing

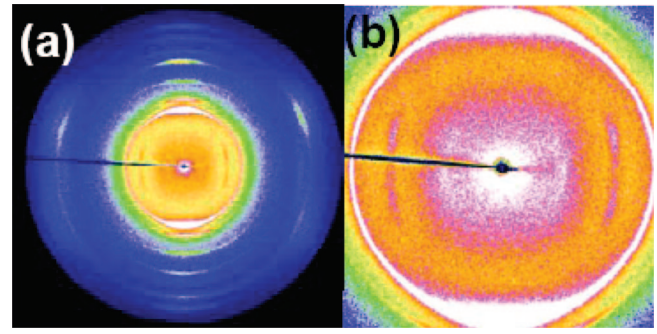

Figure 8. (a) Two-dimensional X-ray fiber diffraction pattern of P(HSe-*co*-55 mol % HA). (b) Partially enlarged diffraction pattern of P(HSe-*co*-55 mol % HA) for the convenience to view the diffractions with small angle.

Table 5. Calculated and Experimental Spacings *d* (nm) of P(HSe-*co*-55 mol % HA) Copolymer[a]

index	d_{calc} (nm)	d_{measd} (nm)	
002	1.07	1.06	w off M
220	0.415	0.416	vs E
040	0.365	0.365	vs E
240	0.296	0.295	m E
400	0.252	0.252	s E
420	0.238	0.238	m E
260	0.219	0.218	w E
440	0.207	0.207	w E
$30\bar{7}$	0.243	0.235	w M
004	0.535	0.535	w off M
$24\bar{7}$	0.222	0.222	w off M
$04\bar{8}$	0.216	0.214	w off M

[a] Based on a monoclinic unit cell with $a = 1.018$ nm, $b = 1.46$ nm, $c = 2.161$ nm, and $\beta = 98°$. Abbreviations denote relative intensities and orientations: vs, very strong; s, strong; m, medium; w, weak; vw, very weak; M, meridional; E, equatorial; off M, off-meridional.

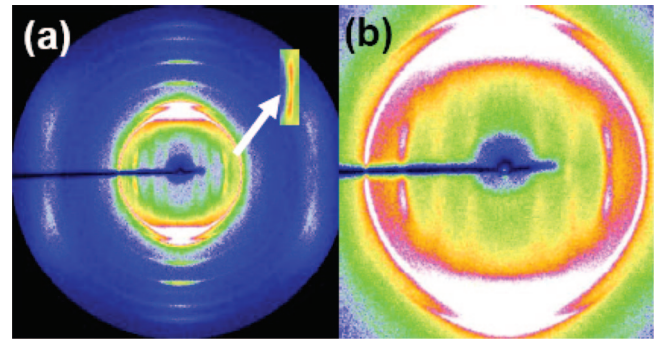

Figure 9. (a) Two-dimensional X-ray fiber diffraction pattern of P(HSe-*co*-75 mol % HA). (b) Partially enlarged diffraction pattern of P(HSe-*co*-75 mol % HA) for the convenience to view the diffractions with small angle.

with 25% HSe comonomer leads to the disappearance of the (003) diffraction peak of PHA, while a new diffraction peak corresponding to a spacing of 0.856 nm in meridional direction appears. The intensity of a diffraction peak corresponding to a spacing of 0.53 nm becomes strong. Some streaks appear in the fiber diffraction pattern of P(HSe-*co*-75 mol % HA), which suggests the formation of defects. The crystal structure of P(HSe-*co*-75 mol % HA) is slightly different from that of PHA. The pattern can be reasonably indexed assuming an orthorhombic unit cell with parameters $a = 1.004$ nm, $b = 1.464$ nm, and $c = 1.712$ nm. The calculated and experimental *d* spacings are listed in Table 6.

For the convenience of comparison, the unit cell parameters of the homopolymers and their copolymers are summarized in Figure 10, which are plotted against the concentration of HA

Table 6. Calculated and Experimental Spacings *d* (nm) of for P(HSe-*co*-75 mol % HA) Copolymer

index	d_{calc} (nm)	d_{measd} (nm)	
002	0.856	0.856	m M
012	0.738	0.735	m off M
102	0.65	0.65	m off M
013	0.532	0.53	s off M
220	0.413	0.414	vs E
040	0.365	0.366	vs E
005	0.342	0.34	vw M
240	0.295	0.295	m E
400	0.25	0.251	m E
420	0.237	0.236	w E
260	0.219	0.22	m E
440	0.206	0.208	w E
027	0.232	0.23	vw M
207	0.22	0.218	w off M
227	0.21	0.211	w off M

[a] Based on an orthorhombic unit cell with parameters $a = 1.004$ nm, $b = 1.464$ nm, and $c = 1.712$ nm. Abbreviations denote relative intensities and orientations: vs, very strong; s, strong; m, medium; w, weak; vw, very weak; M, meridional; E, equatorial; off M, off-meridional.

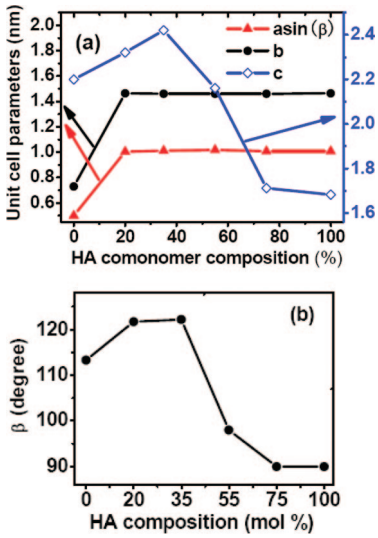

Figure 10. (a) Plot of crystal unit cell parameters $a \sin(\beta)$, b, and c of PHSe, PHA, and P(HSe-*co*-HA) copolymers vs the composition of HA comonomer. (b) Plot of crystal unit cell parameter β of PHSe, PHA, and P(HSe-*co*-HA) copolymers vs the composition of HA comonomer.

comonomer. All copolymers have larger lattice constants c than those of the homopolymers, while lattice constants $a \sin(\beta)$ and b are relatively constant except that of P(HSe-*co*-75 mol % HA). A variation of β exists among P(HSe-*co*-20 mol % HA), P(HSe-*co*-35 mol % HA), and P(HSe-*co*-55 mol % HA), though they all take the monoclinic unit cells.

Discussion

FTIR and X-ray fiber diffraction results revealed that the presence of comonomers leads to formation of new crystal structures, which vary with the concentration of comonomers. Before any detailed analysis of the fiber diffraction patterns, the appearance of new diffraction points suggests the formation of new crystals in the copolymers instead of slight lattice distortion, which generally shifts the diffraction peak position between those of two homocrystals. Further analysis reveals that the copolymers indeed have crystal structures different from the homopolymers, which are also different from each other. P(HSe-*co*-75 mol % HA) adopts an orthorhombic structure, whose lattice constant c is slightly larger than that of PHA, while other copolymers all have monoclinic unit cell, similar to that

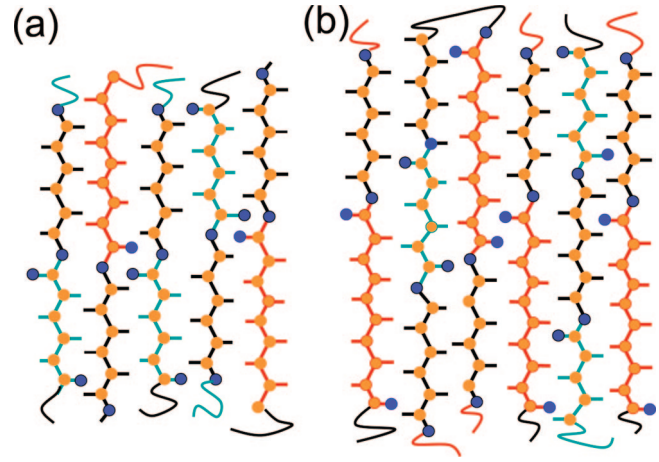

Figure 11. Schematic structures of P(HSe-*co*-20 mol % HA) (a) and P(HSe-*co*-35 mol % HA), P(HSe-*co*-55 mol % HA), and P(HSe-*co*-75 mol % HA) (b). Green, red, and black segment represent a hexanediol acid segment, a sebacic acid segment, and a hexanediol segment, respectively. Croci and blue circle represent a carbon atom and an oxygen atom, respectively.

of PHSe. The lattice constants c of P(HSe-*co*-20 mol % HA) and P(HSe-*co*-35 mol % HA) are larger than those of two homopolymers. In both isomorphism and isodimorphism cases, cocrystallization of copolymers with different comonomer length normally gives the lattice constant c varying inside the window set by two homopolymers, which does not exceed the lattice constant c of the homopolymer with longer monomer length. This seems reasonable as the lattice constant c is generally set by monomer length. Cocrystals can take either individual comonomer lengths or the average value, which will certainly shorter than the long one. Thus, the abnormal large lattice constants c of P(HSe-*co*-20 mol % HA) and P(HSe-*co*-35 mol % HA) suggest a new length scale is induced by the copolymerization, which also supports the formation of new crystal structures rather than normal lattice distortion. Nevertheless, as the copolymerization is statistically random, it is unreasonable to designate a fixed molecular unit for the length scale. A solution is that that part of chain is excluded in the amorphous region.

In the case of P(HSe-*co*-75 mol % HA), the crystal lattice is mainly made up of HA comonomer because HA comonomer is much more than HSe. Some portion of PHSe can squeeze into the unit cell, and others have to be pushed to the outside of the lamellar crystals, as shown in Figure 11a. Because PHSe comonomer can shift along the chain direction, the repetition along the chain direction within the crystal is aperiodic. This nonperiod layer[30] may be hinted by the streaks of the first and second layers in the diffraction pattern of P(HSe-*co*-75 mol % HA) (see Figure 9).

As for P(HSe-*co*-20 mol % HA) and P(HSe-*co*-35 mol % HA), their lattice constants c are one or two C−C bonds longer than PHSe. The crystal lattice is mainly made up of HSe comonomer because HSe comonomer is more than HA. The nature of cocrystallization means that HA comonomer exists in the crystals. A HA comonomer with a adipic acid segment or a hexanediol segment can squeeze in the unit cell though a small portion may be pushed to the outside of the crystal as shown in Figure 11b. As for P(HSe-*co*-55 mol % HA), diffraction patterns show that crystal structure of P(HSe-*co*-55 mol % HA) is similar to that of PHSe, so crystallization is still dominated by HSe comonomer though HA comonomer is more than HSe. Thus, it may belong to the case of P(HSe-*co*-20 mol % HA) and P(HSe-*co*-35 mol % HA).

Excluding part of the molecular chain to the amorphous region is natural as semicrystalline polymers always compose of an interlamellar amorphous layer. The question remaining is whether this is connected with the crystal lattice. Gan et al.[12] reported that the crystals of aliphatic polyester and its copolyesters have a crystal thickness of about 3−5 nm, which is only 2−3 times the lattices constant *c*. Thus, almost every unit cell has a direct connection with amorphous regions. This may allow the crystals to select right lattice constant *c* and then leave part of segment in the amorphous layers. Nevertheless, the choice of lattice constant *c* may also involve internal defects such as disordered conformations which are widely present in the crystals of aliphatic polyesters.[42]

The lattice constants *b* and $a \sin(\beta)$ of PHA and the copolymers crystals are identical except that of PHSe homopolymer (see Figure 10). The crystal structures of PHA and the copolymers take a large unit cell with 8 chains per unit, while the unit cell of PHSe contains only 2 chains. This leads to the large difference between their lattice constants $a \sin(\beta)$ and *b* of PHSe and the copolymers. This suggests that it may be more proper for PHSe to adopt a large unit cell. If the *a* and *b* of PHSe are doubled as the same as PHA and PHS,[33,34] namely $a = 1.088$ and $b = 1.46$ nm, the lattice constants $a \sin(\beta)$ and *b* of PHSe, PHA, and their P(HSe-*co*-HA) copolymers are almost identical.

Because HA and HSe comonomers can cocrystallize in the whole range of copolymer compositions, the volume per non-hydrogen atom inside the unit cell should vary rather slightly and continuously. The volume per non-hydrogen atom inside the unit cell can be described as following equation:

$$V_{\text{atom}} = \frac{V_{\text{cell}}}{N} \tag{1}$$

where *N* is the number of non-hydrogen atom inside the unit cell and V_{cell} is the volume of the unit cell. The volume of the orthorhombic or monoclinic unit cell can be calculated by the following equation:

$$V_{\text{cell}} = abc \sin\beta \tag{2}$$

The number of non-hydrogen atoms inside the unit cell can be estimated by following equation:

$$N = \frac{nc}{d} \tag{3}$$

where *n* is the number of chains inside the unit cell, *c* is the lattice constant of the unit cell, and *d* is projection of the C−C or C−O bond along the *c* axis. Assuming the projections of C−C bond and C−O bond are roughly equal in the *c* axis direction, the monomers of poly(hexamethylene succinate) (PHS), PHA, and PHSe have equivalent lengths of 12, 14, and 18 C−C bonds, respectively. Puiggali et al. have reported the *c* of PHS, PHA, and PHSe were 1.44, 1.683, and 2.2 nm.[33,34,41] An average length of C−C bond in the *c* direction is 0.120, 0.120, and 0.122 nm, respectively. Taken the projection of the length of C−C or C−O bond in the copolymers as 0.120 nm, the volumes per non-hydrogen atom inside the unit cell of PHA, PHSe, and P(HSe-*co*-HA) crystals are almost the same (0.022 nm^3).

Conclusion

On the basis of the characteristic FTIR absorption bands of PHSe and PHA crystals as well as the melting behavior, poly(hexamethylene sebacate-*co*-hexamethylene adipate) P(HSe-*co*-HA) random copolymers form cocrystals in the whole range of composition. X-ray fiber diffraction patterns show that some new diffraction peaks appear, while some diffractions shift slightly off from those of the homopolymers. The diffraction patterns of the copolymers correspond to new crystals with different unit cells from those of the homopolymers. The unit cell parameters are proposed for all copolymers, which are different not only from the homopolymers but also from each other. The lattice constants *c* of P(HSe-*co*-20 mol % HA) and P(HSe-*co*-35 mol % HA) crystals are abnormally larger than those of either homopolymers, which we could not find the corresponding monomer length. A possible solution for this new length scale may be required to consider that part of chain is excluded in the amorphous region.

Acknowledgment. This work is supported by the National Science Foundation (50503015) as well as the "NCET" from the Ministry of Education. The research is also in part supported by the Opening Project of the State Key Laboratory of Polymer Materials Engineering (Sichuan University) and experimental fund of National Synchrotron Radiation Lab.

References and Notes

(1) Chandra, R.; Rustgi, R. *Prog. Polym. Sci.* **1998**, *23*, 1273–1335.
(2) Coulembier, O.; Degée, P.; Hedrick, J. L.; Dubois, P. *Prog. Polym. Sci.* **2006**, *31*, 723–747.
(3) *Biopolymers: Polyesters I*; Doi, Y., Steinbuchel, A., Eds.; Wiley-VCH: Weinheim, 2002; Vol. *3a*.
(4) Ruzette, A. V.; Leibler, L. *Nat. Mater.* **2005**, *4*, 19–31.
(5) Hamley, I. W. *The Physics of Block Copolymers*; Oxford University Press: New York, 2000.
(6) Di Marzio, E. A. *Prog. Polym. Sci.* **1999**, *24*, 329–377.
(7) Muthukumar, M.; Ober, C. K.; Thomas, E. L. *Science* **1997**, *277*, 1225–1232.
(8) Li, L. B.; Meng, F. H.; Zhong, Z. Y.; Byelov, D.; De Jeu, W. H.; Feijen, J. *J. Chem. Phys.* **2007**, *126*, 1–7.
(9) Li, L. B.; Séréro, Y.; Michel, K.; De Jeu, W. H. *Macromolecules* **2003**, *36*, 529–532.
(10) Muller, A. J.; Balsamo, V.; Arnal, M. L. *Adv. Polym. Sci.* **2005**, *190*, 1–63.
(11) Stein, R. S.; Khambatta, F. B.; Warner, F. P.; Russell, T.; Escala, A.; Balizer, E. *J. Polym. Sci., Polym. Symp.* **1978**, *63*, 313–328.
(12) Gan, Z. H.; Abe, H.; Kurokawa, H.; Doi, Y. *Biomacromolecules* **2001**, *2*, 605–613.
(13) Gan, Z. H.; Jiang, B. Z.; Zhang, J. *J. Appl. Polym. Sci.* **1996**, *59*, 961–967.
(14) Kuwabara, K.; Gan, Z. H.; Nakamura, T.; Abe, H.; Doi, Y. *Biomacromolecules* **2002**, *3*, 390–396.
(15) Natta, G.; Corradini, P.; Sianesi, D.; Morero, D. *J. Polym. Sci.* **1961**, *51*, 527.
(16) De Rosa, C.; Talarico, G.; Caporaso, L.; Auriemma, F.; Galimberti, M.; Fusco, O. *Macromolecules* **1998**, *31*, 9109–9115.
(17) Tanakapr, A.; Hozumi, Y.; Hatada, K.; Endo, S.; Fujishige, R. *J. Polym. Sci.* **1964**, *2*, 181.
(18) Guerra, G.; Di Dino, G.; Centore, R.; Petraccone, V.; Obrzut, J.; Karasz, F. E.; MacKnight, W. J. *Makromol. Chem.* **1989**, *190*, 2203–2210.
(19) Kakugo, M. *Macromol. Symp.* **1995**, *89*, 545–552.
(20) Auriemma, F.; De Rosa, C.; Corradini, P. *Adv. Polym. Sci.* **2005**, *181*, 1–74.
(21) Jeong, Y. G.; Jo, W. H.; Lee, S. C. *Macromolecules* **2000**, *33*, 9705–9711.
(22) Lee, J. H.; Jeong, Y. G.; Lee, S. C.; Min, B. G.; Jo, W. H. *Polymer* **2002**, *43*, 5263–5270.
(23) Tashiro, K.; Stein, R. S.; Hsu, S. L. *Macromolecules* **1992**, *25*, 1801–1808.
(24) Tashiro, K.; Satkowski, M. M.; Stein, R. S.; li, Y. J.; Chu, B.; Hsu, S. L. *Macromolecules* **1992**, *25*, 1809–1815.
(25) Tashiro, K.; Izuchi, M.; Kobayashi, M.; Stein, R. S. *Macromolecules* **1994**, *27*, 1234–1239.
(26) Papageorgiou, G. Z.; Bikiaris, D. N. *Biomacromolecules* **2007**, *8*, 2437–2449.
(27) Wendling, J.; Gusev, A. A.; Suter, U. W.; Braam, A.; Leemans, L.; Meier, J. R.; Aerts, J.; Heuvel, J. v. d.; Hottenhuis, M. *Macromolecules* **1999**, *32*, 7866–7878.
(28) Wendling, J.; Suter, U. W. *Macromolecules* **1998**, *31*, 2509–2515.
(29) Wendling, J.; Suter, U. W. *Macromolecules* **1998**, *31*, 2516–2520.
(30) Hanna, S.; Romo-Uribe, A.; Windle, A. H. *Nature (London)* **1993**, *366*, 546–549.
(31) Wendling, J.; Suter, U. W. *Macromol. Theory Simul.* **1999**, *8*, 110–118.
(32) Aylwin, P. A.; Boyd, R. H. *Polymer* **1984**, *25*, 323–329.

(33) Gesti, S.; Almontassir, A.; Casas, M. T.; Puiggali, J. *Biomacromolecules* **2006**, *7*, 799–808.
(34) Armelin, E.; Casas, M. T.; Puiggali, J. *Polymer* **2001**, *42*, 5695–5699.
(35) Gesti, S.; Almontassir, A.; Casas, M. T.; Puiggali, J. *Polymer* **2004**, *45*, 8845–8861.
(36) Almontassir, A.; Gesti, S.; Franco, L.; Puiggali, J. *Macromolecules* **2004**, *37*, 5300–5309.
(37) Pouget, E.; Almontassir, A.; Casas, M. T.; Puiggali, J. *Macromolecules* **2003**, *36*, 698–705.
(38) Iwata, T.; Doi, Y. *Macromol. Chem. Phys.* **1999**, *200*, 2429–2442.
(39) Kuwabara, K.; Gan, Z. H.; Nakamura, T.; Abe, H.; Doi, Y. *Biomacromolecules* **2002**, *3*, 390–396.
(40) Kuwabara, K.; Gan, Z. H.; Nakamura, T.; Abe, H.; Doi, Y. *Biomacromolecules* **2002**, *3*, 1095–1100.
(41) Gesti, S.; Casas, M. T.; Puiggali, J. *Polymer* **2007**, *48*, 5088–5097.
(42) Liau, W. B.; Boyd, R. H. *Macromolecules* **1990**, *23*, 1531–1539.

MA702888D